Досліджено вплив умов електролізу при різних складах електроліту на фазоутворення і властивості покриттів, отриманих мікродуговим оксидуванням (МДО) на алюмінієвому сплаві АМг6. Для електролізу використовувалися електроліти трьох типів: лужний електроліт (розчин (КОН) в дистильованої воді), силікатний електроліт (з різним процентним вмістом Na_2SiO_3 складової) і комплексний лужно-силікатний електроліт з вмістом рідкого скла (1÷12 г/л Na_2SiO_3) і гідроксиду калію (1÷6 г/л КОН). Аналіз отриманих результатів показав, що вибір типу електроліту і умов протікання процесу мікродугового оксидування дозволяє в широких межах змінювати фазово-структурний стан, товщину і властивості алюмінієвого сплаву АМг6. Критерієм очікуваного в результаті мікродугового оксидування фазово-структурного стану покриттів є повнота протікання процесу γ-Al_2O_3→α-Al_2O_3 перетворення при формуванні покриттів. Використання лужного електроліту не дозволяє досягти високої твердості покриття через формування γ-Al_2O_3 фази і відсутності термодинамічних умови для переходу γ-Al_2O_3→α-Al_2O_3. При використанні силікатної електроліту вдається значно підвищити швидкість росту покриття, але при цьому наявність великої питомої концентрації Si стимулює утворення муллиту і аморфноподібної фази. Використання комбінованого лужно-силікатного електроліту (з різним процентним вмістом КОН+Na_2SiO_3) при малому вмісті (6 г/л) Na_2SiO_3 в розчині, стимулює утворення муллиту. Це проявляється в найбільшій мірі при найменшому вмісту (1 г/л) КОН складової. При більшому вмісті (2 г/л) КОН складової, стають домінуючими процеси, які характерні для лужного електроліту. Це призводить до незавершеності реакції перетворення і утворення тільки γ-Al_2O_3 фази. Досягнення термодинамічних умов γ-Al_2O_3→α-Al_2O_3 перетворення стало можливим при збільшенні до 12 г/л питомої вмісту Na_2SiO_3 в розчині електроліту. В цьому випадку формувалися МДО-покриття на сплаві АМг6 з найбільшою твердістю 1500 кг/мм^2 і високою електричною міцністю 12 В/мкм

Ключові слова: мікродугове оксидування, лужний електроліт, силікатний електроліт, комплексний електроліт, фазовий склад, електрична міцність

UDC 539.216.2: 537.52
DOI: 10.15587/1729-4061.2020.205474

A STUDY OF THE ELECTROLYTE COMPOSITION INFLUENCE ON THE STRUCTURE AND PROPERTIES OF MAO COATINGS FORMED ON AMG6 ALLOY

V. Subbotina
PhD, Associate Professor*
E-mail: subbotina.valeri@gmail.com
O. Sobol
Doctor of Physical and Mathematical Sciences, Professor*
E-mail: sool@kpi.kharkov.ua
V. Belozerov
PhD, Professor*
Ubeidulla F.Al-Qawabeha
PhD, Associate Professor**
E-mail: ubeid1@yahoo.com
Taha A.Tabaza
PhD, Associate Professor**
E-mail: safwan1q@gmail.com
Safwan M. Al-Qawabah
PhD, Associate Professor, Dean - Faculty of Engineering and Technology**
E-mail: safwan1q@gmail.com
V. Shnayder
Postgraduate Student*
Email: valikshnayder@gmail.com
*Department of Materials Science
National Technical University "Kharkiv Polytechnic Institute"
Kyrpychova str., 2, Kharkiv, Ukraine, 61002
**Department of Mechanical Engineering, Faculty of Engineering Al-Zaytoonah University
Queen Alia Airport str., 594, Amman, Jordan, 11733

Received date 20.05.2020
Accepted date 16.06.2020
Published date 30.06.2020

1. Introduction

Applying coatings to the surface of materials, as well as adjusting their composition [1, 2] and structure [3, 4] allows the most rational and cost-effective use of the properties of base materials and modified layers. The scientific basis for this is the method of structural surface engineering [5, 6]. Due to the use of the structural surface engineering method, it was possible to achieve uniquely high properties, primarily mechanical ones: hardness, strength, multi-cycle wear resis-

tance [7, 8]. In this case, the greatest effect was shown by surface modification methods based on plasma technologies, as a result of which superhard coatings were created from new materials [9, 10] or the structure of the base material was modified [11].

One of the most promising plasma technologies, which allows both base material modification and coating formation, is microarc oxidation (MAO). In the literature, this technology is also called: plasma electrolytic oxide (PEO) [12, 13] or anodic spark deposition (ASD) [14]).

Microarc oxidation allows one to obtain multifunctional ceramic-like modified layers (coatings) with a wide range of properties, including high wear resistance, corrosion resistance, heat resistance, and also with good electrical insulating and decorative properties [15, 16].

A distinctive feature of microarc oxidation is the participation of surface microdischarges in the modification process, which have a very significant and specific effect on phase and structure formation. As a result, the composition and structure of the obtained oxide layers are significantly different, and their properties are significantly higher compared to traditional anodizing [17, 18].

In general, MAO is a complex process of electrochemical oxidation in the mode of electric discharge. The characteristics of the resulting coatings depend on many factors. These factors can be attributed to two types, called: external and internal. External factors include (composition and temperature of the electrolyte; electrical parameters – voltage, frequency and shape of pulses, cathodic and anodic current densities, process duration), and internal factors include (alloy composition and heat treatment, surface roughness, base porosity) [19, 20]. These factors determine such characteristics of MAO-modified surfaces as the integral thickness and thickness of individual layers, elemental and phase composition, structure and density of modified layers [21, 22]. Also, the choice of technological regimes for the formation of MAO coatings determines their porosity and corrosion-protective ability, microhardness and wear resistance, adhesion to the base, thermal and electrical conductivity, breakdown voltage, and other properties [23, 24].

The MAO treatment of aluminum alloys allows the formation of coatings with a large thickness (usually up to 400 μm), firmly bonded to the base, consisting of various polymorphic forms of aluminum oxide [25, 26], spinel and other complex oxides. To achieve high properties, the layer of MAO coatings on aluminum alloys, as a rule, should include corundum – α-Al_2O_3, which has high hardness and provides good wear resistance [27, 28]. Such aluminum alloys with MAO coating also have high wear resistance during sliding friction [29, 30]. This makes the development of the scientific foundations of structural engineering for microarc oxidation technology relevant and in demand by modern industry.

2. Literature review and problem statement

The mechanism of microarc oxidation of aluminum and its alloys proceeds with the simultaneous formation and dissolution of aluminum oxide (Al_2O_3) [31]. During the oxidation process, pores filled with electrolyte are formed, which leads to the formation of new regions from aluminum oxides, which subsequently grow with the formation of amorphous layers [32]. Such a mechanism involves the formation of oxide through the transport of oxygen ions (O^{2-}) to the oxide/electrolyte interface and the transfer of Al^{3+} to the metal/oxide interface in the opposite direction [33, 34].

Thus, the electrolyte type has a strong effect on the characteristics of MAO coatings [35]. The composition, concentration and temperature of electrolytes affect the structure, elemental and phase composition of the coatings and, as a consequence, their properties, thickness, change in the initial dimensions of the parts and the rate of formation of the oxide layer. In this regard, modification of the electrolyte composition is another effective way to optimize the microstructure and composition of MAO coatings to improve their properties [36, 37].

Four different compositions based on solutions of silicates and phosphates were used in [38] to study the effect of the electrolyte composition on the phase-structural state and properties of MAO coatings. It was found that coatings obtained in a silicate electrolyte have a more uniform morphology than coatings obtained in a phosphate system. In [39], a combination of KOH with different components (Na_2SiO_3, Na_3PO_4, and $NaAlO_2$) was used as an electrolyte. The results showed that various anions, i. e. SiO_3^{2-}, PO_4^{3-} and AlO^{2-}, affect the characteristics of the coating, such as thickness, chemical composition and structure of the coating. In [40], sodium phosphate, sodium silicate, aluminate, and composite (Na_3PO_4+Na_2SiO_3+$NaAlO_2$) were used for MAO treatment. It was found that the use of different electrolytes leads to different surface porosities of the coatings, with better properties for the sodium phosphate electrolyte. Much attention is also paid to the influence of the electrolyte composition on the microarc oxidation process in many other works [41–43].

Thus, as can be seen from the literature review, the question of the effect of the electrolyte composition on the quality of the MAO coating remains relevant and is widely discussed in periodicals. It should be noted that in most works, data on the phase-structural state have not been systematically studied. And such studies are especially important for determining patterns in the selection of the necessary electrolyte in relation to materials consisting of several elements (for example, alloys). Also, systematic studies on the effect of electrolyte composition and treatment conditions on the quantitative ratio of various phases and their distribution over the coating thickness are important for determining the scientific basis for the mechanism of formation of MAO coatings. This will allow you to control this process and obtain coatings with the necessary structure and properties.

3. The aim and objectives of the study

The aim of the study was to study the phase formation processes in MAO coatings formed on the AMg6 alloy under various electrolysis conditions in alkaline, silicate and alkaline silicate electrolytes and to analyze the influence of the structural features of the coating on their properties.

To achieve this AIM, the following objectives were set:

– to study the effect of different concentrations of alkaline electrolyte (potassium hydroxide solution (KOH) without silicate) on the phase composition and hardness of MAO coatings on the AMg6 alloy;

– to determine the dependence of the formation mechanism of the MAO coating on changes in the content of liquid glass in the electrolyte;

– to determine the effect of the combined (consisting of liquid glass (1÷12 g/l Na_2SiO_3) and potassium hydroxide (1÷6 g/l KOH)) electrolyte on the phase composition, hardness and electric strength of the coatings formed in this electrolyte.

4. Material and methodology for studying the effect of electrolyte composition on the phase-structural state and properties of MAO coatings

Samples in the form of cylinders with a diameter of 25 mm and a height of 10 mm were subjected to MAO treatment. The processed material corresponds to the aluminum alloy AMg6 (Mg – 5.79 %, Mn – 0.74 %, Si – 0.15 %, Ti – 0.04 %, Fe – 0.35 %). Microarc oxidation was carried out in a 100 liter bath. During the MAO process, cooling and sparging of the electrolyte were ensured. The average voltage value was 380 V. The initial current density was 20 A/dm^2, and the treatment time varied.

As electrolytes, the following were used:

1) Alkaline electrolyte – a solution of potassium hydroxide (KOH) in distilled water.

2) Silicate electrolyte (with different percentages of Na_2SiO_3).

3) Combined alkaline silicate electrolyte (with different percentages of KOH+Na_2SiO_3).

The power source used in the work provided the following operating modes:

– 50 Hz alternating current, the ratio of the anode and cathode component of the current I_a/I_c=1 (capacitor type source);

– pulse current – a power source that allows you to receive bipolar voltage pulses of a rectangular shape and provides for the adjustment of the duration of each of them. The frequency and amplitude of the voltage pulses were also regulated.

The following were studied: kinetics of coating formation, phase composition, coating thickness, microhardness and dielectric strength.

Determination of the phase composition of the MAO coatings was carried out according to the results of X-ray phase analysis. The studies were carried out on the DRON-3 installation (Burevesnik, Russia) in monochromatized K_α–Cu radiation. Diffraction spectra were recorded according to the Bragg-Brentano reflection scheme [44]. The shooting was carried out both in continuous and in point-by-point mode with a step of 2θ=0.1°. The maximum error in determining the content of structural crystalline components (with the detectability of 10 vol. %) does not exceed ±0.7 %. The minimum detectability of structural components is about 1 vol. %.

For quantitative phase analysis, the method of reference mixtures was used [45].

The coating thickness was determined on a VT-10 NTs device (Kontrolpribor, Russia). The error in measuring the thickness of the coating is not more than 5 % with the smallest coating thickness (about 10 microns). With a larger coating thickness, the accuracy of determining the thickness increases (for example, with a thickness of 50 μm, the measurement error is not more than 2 %).

Microhardness was determined on a PMT-3 instrument (AO LOMO, Russia). The electric strength (E) was determined by the breakdown voltage at the Universal breakdown installation UPU – 1M (MNIPI, Russia). Technical characteristics of the UPU-1M device: the main limit of the output voltage: 0–10,000 V, auxiliary limits: 0–3,000 V and 0–1,000 V.

5. Results of studying the phase-structural state and surface properties of the AMg6 alloy after MAO treatment in different types of electrolytes

5. 1. MAO treatment in alkaline electrolyte

Alkaline electrolyte is a solution of potassium hydroxide (KOH) in distilled water. The addition of KOH provides the conductivity of the electrolyte. However, its high concentration determines the aggressiveness of the electrolyte, which is manifested in the etching of the surface of the processed material and the forming coating. Therefore, the concentration of KOH in the electrolyte was in the range from 2 to 10 g/l. In addition, as a result of the electrochemical dissociation of KOH, the formed OH^- anions are one of the main electron sources that are necessary for local microarc discharges during the MAO process.

The electrolysis conditions, phase composition and properties of the coatings on the AMg6 alloy are given in Table 1.

Table 1

Characterization of MAO coatings on the AMg6 alloy formed in an alkaline electrolyte

Electrolyte	Treatment time, min	Thickness, μm	Phase composition	HV, kg/mm^2	E, V/μm
KOH-1g/l	60	80	100 % γ-Al_2O_3	1,180	12.0
KOH-2 g/l	60	130		1,150	12.5
KOH-5 g/l	60	100		1,200	12.0

The final anode voltage of microarc oxidation (Fig. 1) depends on the KOH concentration, due to a decrease in the ohmic resistance of the electrolyte. An increase in voltage ensures the process in the microarc discharge mode and an increase in the coating thickness (Fig. 2). The extreme form of the dependence of the coating thickness on the concentration of potassium hydroxide is due to two factors: on the one hand, an increase in the conductivity of the electrolyte and an increase in the thickness of the coating, and on the other hand, chemical dissolution of the coating in an alkaline medium, leading to a decrease in the thickness.

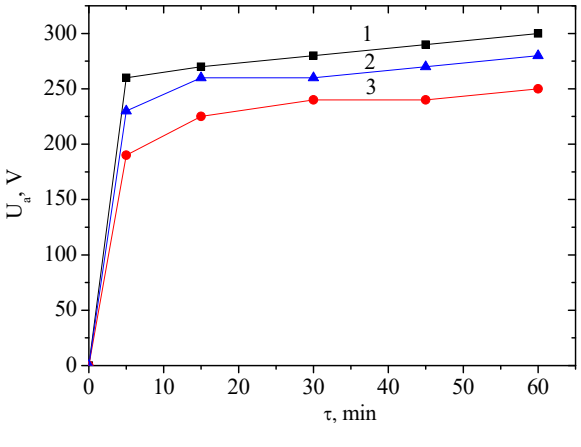

Fig. 1. Chronogram of the anode voltage during the formation of the AMg6 alloy in an aqueous KOH solution, g/l: 1 – 1 g/l; 2 – 2 g/l; 3 – 5 g/l

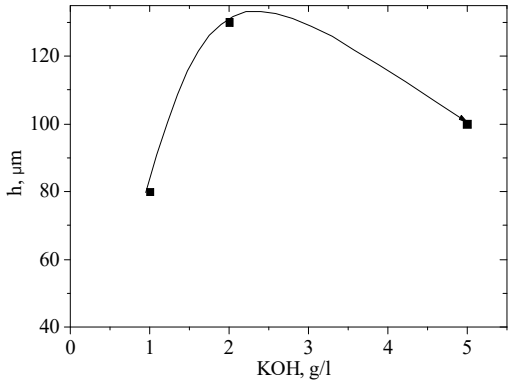

Fig. 2. Thickness of the MAO coatings formed in an alkaline electrolyte (j=20 A/dm^2, τ=60 min)

During MAO treatment of the AMg6 alloy in an alkaline electrolyte, it was revealed that when the coating thickness reaches ~90÷100 μm, discharges appear that cannot be classified as microarc. The power of such discharges is sufficient for melting the coating and forming craters up to the base.

The results obtained indicate satisfactory coating properties (Table 1), hardness is 1,100-1,200 kg/mm^2, which does not always satisfy the requirements for parts working in friction units.

As noted above, the properties of the MAO coatings are determined by their phase composition. The performed X-ray phase analysis showed the following (Fig. 3):

– the coating has a crystalline structure;

– the coating structure is single-phase and corresponds to the γ-Al_2O_3 phase;

– no explicit texture was detected;

– the uniformity of the phase composition is maintained throughout the thickness of the coating.

It should be noted that the diffraction patterns (Fig. 3) contain diffraction reflections corresponding to the aluminum substrate. This is due both to the relatively small coating thickness (the thickness of the semi-absorbing layer of the γ-Al_2O_3 phase is ~50 μm in copper radiation) and to the high porosity of the coatings.

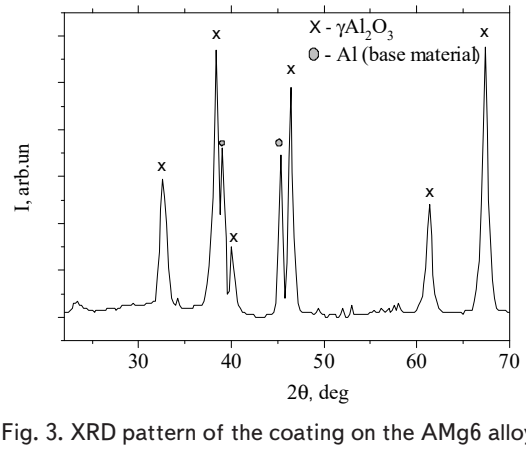

Fig. 3. XRD pattern of the coating on the AMg6 alloy (K_α – Cu radiation, electrolyte – 5 g/l KOH)

Thus, during the electrolysis of the AMg6 alloy in an alkaline electrolyte (1÷5 g/l KOH), the coating mass is aluminum oxide in the form of a crystalline γ-Al_2O_3 phase obtained by electrochemical oxidation of aluminum. Note that the results of the study showed that under the used electrolysis conditions (Table 1), the thermodynamic conditions that ensure the synthesis of α-Al_2O_3 (corundum) by converting γ-Al_2O_3 to α-Al_2O_3 are not achieved.

As a rule, the phase composition of the MAO coatings varies along the layer thickness, which is explained by the inhomogeneity of the temperature field over the coating thickness. However, the absence of the α-Al_2O_3 phase in the coating on the AMg6 alloy is possibly associated not only with the temperature conditions of coating formation. The most probable reason for this phase composition of the coating is the influence of the base and electrolyte components on the structure of the initial γ-Al_2O_3 phase, which leads to its stabilization and the inability of the polymorphic conversion of γ to α.

5. 2. MAO treatment in silicate electrolyte

In terms of technology and ecology of the coating, an aqueous solution of sodium or potassium water glass is promising. Sodium liquid glass was used (state standard 13078-81), the concentration of which varied in the range of 10–50 g/l.

The characteristics of the studied samples and their properties after MAO treatment with silicate electrolyte are given in Table 2.

Table 2

Characterization of MAO coatings on an AMg6 alloy formed in a silicate electrolyte

Electrolyte	τ, min	h, μm	Phases, %				HV, kg/mm^2	E, V/μm
			α	Γ	M	AF		
10 g/l Na_2SiO_3	30	30	–	100	–	–	1,000	11.5
	60	90	–	80	5	15	700	6.6
	120	150	–	70	10	20	1,300	6.3
25 g/l Na_2SiO_3	30	120	–	15	5	80	300	7.2
	60	180	–	30	20	50	660	6.6
	120	220	4	86	10	–	1,080	5.5
50 g/l Na_2SiO_3	5	60	–	3	–	97	–	3.7
	15	180	–	–	–	100	–	3.1
	30	250	–	–	–	100	–	3.0

Note: τ – treatment time, h – total thickness, α – α-Al_2O_3 (corundum), γ – γ-Al_2O_3, M – $3Al_2O_3{\cdot}2SiO_2$ (mullite), AF – X-ray amorphous phase, HV – microhardness, E – electric strength

Data from Table 2 show that at the lowest silicate (Na_2SiO_3) content in the electrolyte, an increase in the oxidation time leads to the appearance of an amorphous phase and mullite. At the highest concentration of silicate in the solution (50 g/l Na_2SiO_3), an amorphous phase is formed in the entire time range, although the growth rate of the coating at this content is the greatest. The highest content of the main components of α-Al_2O_3 and γ-Al_2O_3 is formed at an average concentration of silicate in the solution (25 g/l Na_2SiO_3). Thus, for one type of solution, a large difference in phase composition from silicate concentration can be achieved. The dependence of the percentage of useful α-Al_2O_3 and γ-Al_2O_3 phases on the composition is nonlinear.

Chronograms of the anode current are shown in Fig. 4. The obtained chronograms indicate that the sparking voltage and the final anode voltage of the formation depend on the content of liquid glass. With an increase in the content of liquid glass, a significant decrease in the anode voltage oc-

curs, but this leads to a change in the kinetics of the process and the formation of an amorphous state with low functional properties.

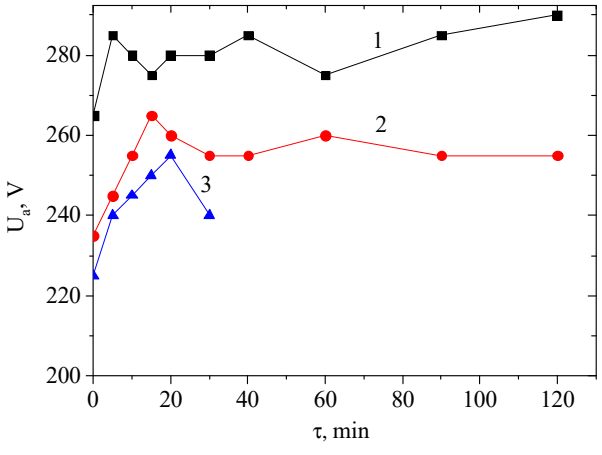

Fig. 4. Chronogram of the anode voltage during coating formation on the AMg6 alloy in a silicate electrolyte: 1 – 10 g/l Na_2SiO_3; 2 – 25 g/l Na_2SiO_3; 3 – 50 g/l Na_2SiO_3

The effect of water glass concentration on the coating thickness is shown in Fig. 5, the kinetics of coating thickness formation for electrolytes with different liquid glass contents is shown in Fig. 6.

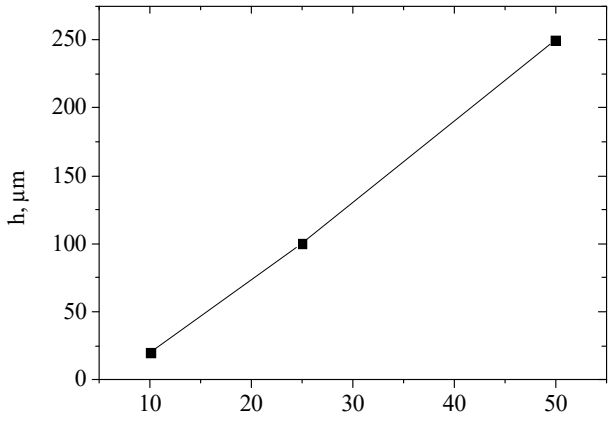

Fig. 5. Effect of water glass on the coating thickness (AMg6 alloy; treatment time – 30 min)

Thus, the analysis of the results presented (Fig. 4–6, Table 2) indicates that an increase in the liquid glass concentration reduces the voltage of coating formation (Fig. 4). However, the high rate (kinetics) of the process (Fig. 5, 6) does not allow the crystalline phase to form.

In this case, the main component is X-ray amorphous, which manifests itself in the diffraction spectrum (Fig. 7) as the formation of a diffuse diffraction region in the angular range of 2θ≈14...35 degrees (indicated in Fig. 7 as a "halo").

A similar "halo" (however, significantly smaller in relative volumetric content) is detected in a similar angular interval and in the spectrum from the coating obtained at a lower Na_2SiO_3 content (Fig. 8). If we assume that the appearance of a "halo" in the spectrum is associated with the formation of a nano-cluster structural state, then the average position of the maximum corresponds to an angle of 2θ=22.1 degrees, which does not coincide with the position of the diffraction peaks from the assumed phases. Such an effect of displacement and smearing in a large angular range of the diffraction maximum can be associated with very small sizes of the ordering regions (almost no long-range order in the arrangement of atoms). If we assume that the appearance of a diffuse halo diffraction region is associated with the small size of the ordering regions (nano-cluster type), then, based on the half-width of the halo, the size of such regions is about 1.2 nm. In addition, in the diffraction spectrum of Fig. 7, there are 3 diffraction peaks from the base (aluminum) material and a low intensity peak in the region of 2θ≈23 deg., the appearance of which can be associated with the onset of crystallization of the γ-Al_2O_3 phase.

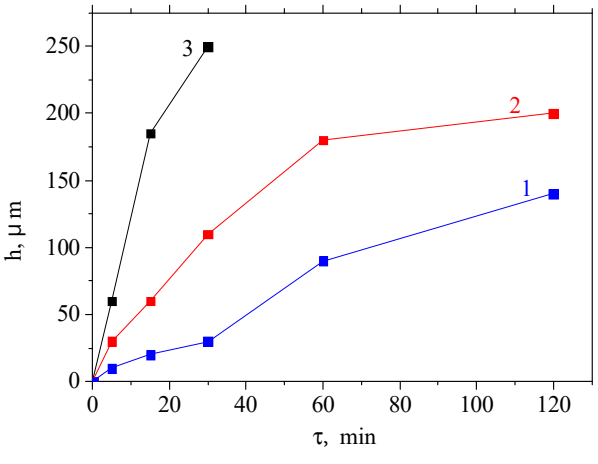

Fig. 6. Kinetics of coating thickness formation on the AMg6 alloy: 1 – 10 g/l Na_2SiO_3; 2 – 25 g/l Na_2SiO_3; 3 – 50 g/l Na_2SiO_3

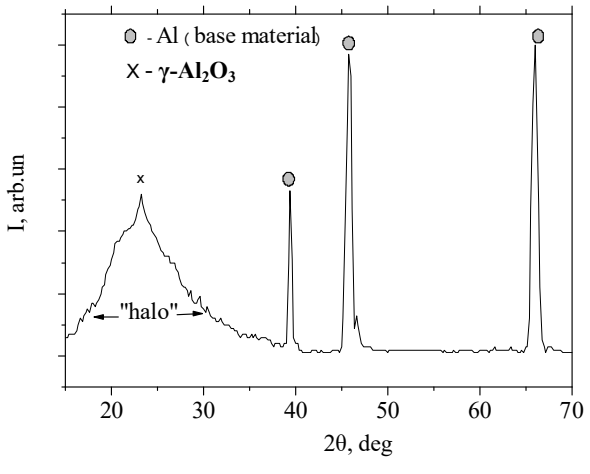

Fig. 7. Diffraction pattern of the coating on the AMg6 alloy: K_α – Cu radiation, electrolyte – 50 g/l Na_2SiO_3

At a lower content of the Na_2SiO_3 component, although the rate of coating formation decreases, the formation of the crystalline γ-Al_2O_3 phase is observed (Fig. 8).

The results obtained indicate that, depending on the silicate concentration, the relationship between electrochemical and electrophoretic processes changes. In dilute solutions, the bulk of the coating is Al_2O_3 in amorphous or crystalline form, and in concentrated solutions with a high Na_2SiO_3 content, the relative Si content in the electrolyte increases,

which leads to the predominant coating formation due to the SiO_2 (silica) phase. This leads to amorphization of the coating structure and a decrease in functional properties. Thus, there is a redistribution of the two components of the mullite Al_2O_3 and SiO_2 depending on the content of Na_2SiO_3.

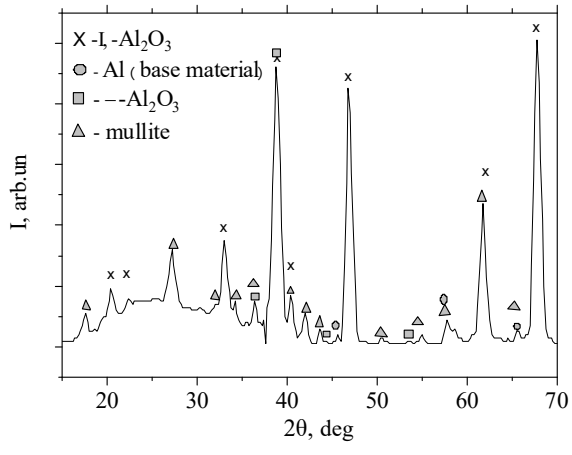

Fig. 8. Diffraction pattern of the coating on the AMg6 alloy: K_α – Cu radiation, electrolyte – 10 g/l Na_2SiO_3, h=60 μm

Moreover, based on the results obtained, in solutions with the lowest liquid glass content (highly diluted solutions), a mixed coating formation mechanism takes place. In this case, the formation of the γ–Al_2O_3 modification occurs by the electrochemical method, and the formation of SiO_2 by – the electrophoretic one [46].

It should be noted that the phase composition over the coating thickness is heterogeneous (Fig. 9, 10, Table 2). This fact can be explained by the heterogeneity of the temperature field in the coating and the change in the ratio of the coating formation mechanisms during growth.

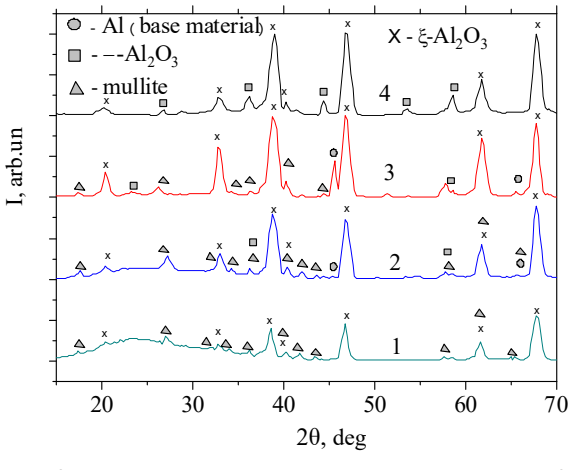

Fig. 9. Diffraction patterns of the coating on the AMg6 alloy – results of layer-by-layer analysis: K_α – Cu radiation, electrolyte – 25 g/l Na_2SiO_3, h=200 μm; 1 – h=200 μm (surface); 2 – h=160 μm; 3 – h=110 μm; 4 – h=50 μm (separated coating)

As can be seen from Fig. 10, the highest relative content of α-Al_2O_3 is near the substrate. Also, near the substrate, there is the highest relative content of the γ-Al_2O_3 phase. The amorphous phase and mullite are predominantly located near the surface of the coating, and near the substrate their content is almost close to zero. Thus, to achieve the highest operational characteristics, you should remove the surface layer with a thickness of about 130...150 microns. In this case, practically only α-Al_2O_3 and γ-Al_2O_3 phases will be contained in the remaining coating with a thickness of about 100 nm.

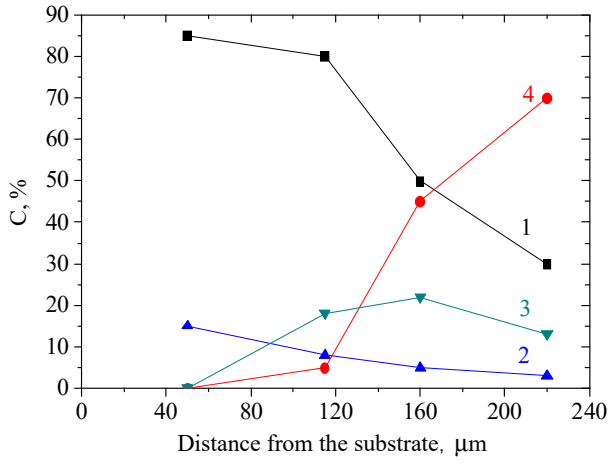

Fig. 10. Phase composition by coating thickness: 1 – γ-Al_2O_3, 2 – α-Al_2O_3, 3 – $3Al_2O_3{\cdot}2SiO_2$, 4 – amorphous phase

5. 3. MAO treatment in an alkaline silicate electrolyte

As the results of sections 5. 1 and 5. 2 showed, individually, neither alkaline nor silicate electrolyte can achieve high functional properties. When using an alkaline electrolyte, a relatively low coating formation rate is accompanied by the formation of the γ-Al_2O_3 phase (Table 1). When using a silicate electrolyte, a significant increase in the growth rate of the coating occurs, however, the formation of an amorphous-like state, whose functional properties are also not high, becomes kinetically beneficial (Table 2). Therefore, a study was conducted of the MAO treatment in a complex electrolyte containing solutions of sodium silicate and potassium hydroxide.

The characteristics of coatings on the AMg6 alloy formed in alkaline silicate electrolytes used in this work are given in Table 3.

Table 3

Phase composition, hardness and dielectric strength of coatings on AMg6 alloy

Electrolyte	τ, min	h, μm	Phases, %			HV, kg/mm^2	E, V/μm
			α	γ	M		
1 g/l KOH+ +6 g/l Na_2SiO_3	60	70	–	96	4	1,480	12.0
	120	120	–	85	15	1,400	11.8
	180	200	–	70	30	1,400	12.0
2 g/l KOH+ +6 g/l Na_2SiO_3	60	44	–	100	–	1,100	11.5
	120	83	–	100	–	1,180	12.0
	180	116	–	100	–	1,200	12.0
2 g/l KOH+ +12 g/l Na_2SiO_3	60	91	–	100	-	1,150	11.5
	120	130	-	80	20	1,480	11.5
	180	220	25	55	20	1,500	12.0

Note: τ – treatment time, h – total thickness, α – α-Al_2O_3 (corundum), γ – Al_2O_3, M – $3Al_2O_3{\cdot}2SiO_2$ (mullite), HV – microhardness, E – electric strength

As can be seen from Table 3, in almost all the studied electrolytes, a coating is formed, consisting mainly of the

crystalline phase γ-Al_2O_3. It should be noted that in the process of coating formation, the process begins with the formation of the γ-Al_2O_3 phase, the next stage is the formation of mullite ($3Al_2O_3{\cdot}2SiO_2$) and the last stage is the formation of the α-Al_2O_3 phase (corundum) as a result of the transformation process: γ-$Al_2O_3 \rightarrow \alpha$-$Al_2O_3$.

6. Discussion of the effects of different types of electrolytes on the phase-structural state and properties of MAO coatings on the AMg6 alloy

An analysis of the results shows that the choice of electrolyte type and conditions of the microarc oxidation process can significantly change the phase-structural state and surface properties (while achieving the best properties with a modified surface layer thickness of about 100...200 μm) of the AMg6 aluminum alloy. In addition, as can be seen from Fig. 10, the composition and properties of MAO coatings are largely dependent on its thickness.

The criterion for the expected phase-structural state of the coatings as a result of microarc oxidation is the completeness of the γ–$Al_2O_3 \rightarrow \alpha$–$Al_2O_3$ transformation process during coating formation.

The use of an alkaline electrolyte ((KOH) solution in distilled water) does not allow achieving a high hardness of the coating due to the formation of the γ-Al_2O_3 phase and the absence of thermodynamic conditions for the γ–$Al_2O_3 \rightarrow \alpha$–$Al_2O_3$ transition.

When using a silicate electrolyte (with different percentages of Na_2SiO_3), it is possible to significantly increase the growth rate of the coating, but the presence of a large specific Si concentration stimulates the formation of mullite and an amorphous-like phase (Table 2, Fig. 7). In this case, the surface layer contains the largest specific volume of mullite and amorphous-like phase, which makes it porous and with low hardness. At the same time, in the region close to the base material, the formation of α-Al_2O_3 and γ-Al_2O_3 phases occurs (Fig. 10). This is apparently a consequence of an increase in the temperature in the breakdown channels, which leads to the interaction of Al_2O_3 and SiO_2 with the formation of mullite ($3Al_2O_3{\cdot}2SiO_2$). The formation of the α-Al_2O_3 (corundum) phase by the polymorphic transformation γ–$Al_2O_3 \rightarrow \alpha$–$Al_2O_3$ requires special thermodynamic conditions that are satisfied only near the base material. In this case, the kinetics of the process allows the γ–$Al_2O_3 \rightarrow \alpha$–$Al_2O_3$ transition to occur only at an average concentration (25 g/l) of the Na_2SiO_3 component (Table 2).

Using a combined alkaline silicate electrolyte (with different percentages of KOH+Na_2SiO_3) allowed us to achieve the thermodynamic conditions of the γ–$Al_2O_3 \rightarrow \alpha$–$Al_2O_3$ transformation only at a relatively high (12 g/l) Na_2SiO_3 content (Table 3).

At a lower content (6 g/l), the presence of Na_2SiO_3 in the solution stimulates the formation of mullite. This is manifested to the greatest extent with the smallest (1 g/l) content of the KOH component in the solution. At a higher content (2 g/l) of KOH, the processes characteristic of an alkaline electrolyte become dominant (Table 1), which leads to incomplete conversion reactions and the formation of only the γ-Al_2O_3 phase. Only an increase in the specific Na_2SiO_3 content to 12 g/l allows us to create thermodynamic conditions for the γ–$Al_2O_3 \rightarrow \alpha$–$Al_2O_3$ transformation and the formation of a solid layer (1500 kg/mm^2) with high electric strength.

Thus, an analysis of the results made it possible to find out that only the use of a complex electrolyte allows one to create thermodynamic conditions for the γ–$Al_2O_3 \rightarrow \alpha$–$Al_2O_3$ conversion reaction and the formation of a highly solid α-Al_2O_3 phase. Therefore, further studies suggest the determination of structural-phase transformations of the MAO coatings obtained in complex electrolytes with a high content of Na_2SiO_3 component. Such studies are important, since in this case there are limitations associated with a decrease in crystallite sizes up to the achievement of an amorphous-like state. This can lead to a decrease in the physicomechanical characteristics of such MAO coatings.

7. Conclusions

1. It is found that the phase composition of the coating is determined by the coating formation mechanism. In the absence of silicate in the electrolyte, an electrolytic coating formation mechanism is implemented. The phase composition of the coating is the γ-Al_2O_3 phase with a hardness of 1,200 kg/mm^2.

2. A significant influence on the mechanism and processes of coating formation is made by the addition of water glass in the electrolyte. At a low content of liquid glass (10 g/l Na_2SiO_3), the electrolytic mechanism of coating formation is realized, and at high (50 g/l Na_2SiO_3), an electrophoretic mechanism is realized, which leads to the formation of an X-ray amorphous phase with a reduced hardness.

3. MAO coatings on an AMg6 alloy with the highest hardness of 1,500 kg/mm^2 and high electric strength of 12 V/μm were obtained in combined electrolytes consisting of liquid glass (1÷12 g/l Na_2SiO_3) and potassium hydroxide (1÷6 g/l KOH). This became possible due to the formation of α-Al_2O_3 and γ-Al_2O_3 phases in such an electrolyte and the absence of an amorphous state.

8. Acknowledgments

The authors would like to express their gratitude to the Ministry of Education and Science of Ukraine for financial support in the framework of the project “Development of material science for the use of high-performance ion-plasma technologies for three-level surface engineering” (state registration number No. 0118U002044), as well as to the Al-Zaytoonah University of Jordan for financial support under the project (19/18/2018-2019)

References

1. Fedirko, V. M., Pohrelyuk, I. M., Luk’yanenko, O. H., Lavrys’, S. M., Kindrachuk, M. V., Dukhota, O. I. et. al. (2018). Thermodiffusion Saturation of the Surface of VT22 Titanium Alloy from a Controlled Oxygen–Nitrogen-Containing Atmosphere in the Stage of Aging. Materials Science, 53 (5), 691–701. doi: https://doi.org/10.1007/s11003-018-0125-z

2. Sobol, O. V., Postelnyk, A. A., Meylekhov, A. A., Andreev, A. A., Stolbovoy, V. A., Gorban, V. F. (2017). Structural Engineering of the Multilayer Vacuum Arc Nitride Coatings Based on Ti, Cr, Mo and Zr. Journal of Nano- and Electronic Physics, 9 (3), 03003-1–03003-6. doi: https://doi.org/10.21272/jnep.9(3).03003
3. Vereschaka, A., Grigoriev, S., Tabakov, V., Migranov, M., Sitnikov, N., Milovich, F., Andreev, N. (2020). Influence of the nanostructure of Ti-TiN-(Ti,Al,Cr)N multilayer composite coating on tribological properties and cutting tool life. Tribology International, 150, 106388. doi: https://doi.org/10.1016/j.triboint.2020.106388
4. Sobol', O. V., Andreev, A. A., Gorban', V. F., Stolbovoy, V. A., Melekhov, A. A., Postelnyk, A. A. (2016). Possibilities of structural engineering in multilayer vacuum-arc ZrN/CrN coatings by varying the nanolayer thickness and application of a bias potential. Technical Physics, 61 (7), 1060–1063. doi: https://doi.org/10.1134/s1063784216070252
5. Morton, B. D., Wang, H., Fleming, R. A., Zou, M. (2011). Nanoscale Surface Engineering with Deformation-Resistant Core–Shell Nanostructures. Tribology Letters, 42 (1), 51–58. doi: https://doi.org/10.1007/s11249-011-9747-0
6. Sobol, O. V., Andreev, A. A., Gorban, V. F., Meylekhov, A. A., Postelnyk, H. O., Stolbovoy, V. A. (2016). Structural Engineering of the Vacuum Arc ZrN/CrN Multilayer Coatings. Journal of Nano- and Electronic Physics, 8 (1), 1042-1–1042-5. doi: https://doi.org/10.21272/jnep.8(1).01042
7. Sobol', O. V., Meilekhov, A. A. (2018). Conditions of Attaining a Superhard State at a Critical Thickness of Nanolayers in Multiperiodic Vacuum-Arc Plasma Deposited Nitride Coatings. Technical Physics Letters, 44 (1), 63–66. doi: https://doi.org/10.1134/s1063785018010224
8. Lackner, J., Waldhauser, W., Major, L., Kot, M. (2014). Tribology and Micromechanics of Chromium Nitride Based Multilayer Coatings on Soft and Hard Substrates. Coatings, 4 (1), 121–138. doi: https://doi.org/10.3390/coatings4010121
9. Sobol', O. V., Andreev, A. A., Gorban', V. F. (2016). Structural Engineering of Vacuum-ARC Multiperiod Coatings. Metal Science and Heat Treatment, 58 (1-2), 37–39. doi: https://doi.org/10.1007/s11041-016-9961-3
10. Veprek, S., Veprek-Heijman, M. G. J., Karvankova, P., Prochazka, J. (2005). Different approaches to superhard coatings and nanocomposites. Thin Solid Films, 476 (1), 1–29. doi: https://doi.org/10.1016/j.tsf.2004.10.053
11. Kim, M. C., Yang, S. H., Boo, J.-H., Han, J. G. (2003). Surface treatment of metals using an atmospheric pressure plasma jet and their surface characteristics. Surface and Coatings Technology, 174-175, 839–844. doi: https://doi.org/10.1016/s0257-8972(03)00560-7
12. Arrabal, R., Matykina, E., Hashimoto, T., Skeldon, P., Thompson, G. E. (2009). Characterization of AC PEO coatings on magnesium alloys. Surface and Coatings Technology, 203 (16), 2207–2220. doi: https://doi.org/10.1016/j.surfcoat.2009.02.011
13. Agureev, L., Savushkina, S., Ashmarin, A., Borisov, A., Apelfeld, A., Anikin, K. et. al. (2018). Study of Plasma Electrolytic Oxidation Coatings on Aluminum Composites. Metals, 8 (6), 459. doi: https://doi.org/10.3390/met8060459
14. Curran, J. A., Kalkancı, H., Magurova, Y., Clyne, T. W. (2007). Mullite-rich plasma electrolytic oxide coatings for thermal barrier applications. Surface and Coatings Technology, 201 (21), 8683–8687. doi: https://doi.org/10.1016/j.surfcoat.2006.06.050
15. Yerokhin, A. L., Nie, X., Leyland, A., Matthews, A., Dowey, S. J. (1999). Plasma electrolysis for surface engineering. Surface and Coatings Technology, 122 (2-3), 73–93. doi: https://doi.org/10.1016/s0257-8972(99)00441-7
16. Subbotina, V., Al-Qawabeha, U. F., Belozerov, V., Sobol, O., Subbotin, A., Tabaza, T. A., Al-Qawabah, S. M. (2019). Determination of influence of electrolyte composition and impurities on the content of α-AL2O3 phase in MAO-coatings on aluminum. Eastern-European Journal of Enterprise Technologies, 6 (12 (102)), 6–13. doi: https://doi.org/10.15587/1729-4061.2019.185674
17. Curran, J. A., Clyne, T. W. (2005). Thermo-physical properties of plasma electrolytic oxide coatings on aluminium. Surface and Coatings Technology, 199 (2-3), 168–176. doi: https://doi.org/10.1016/j.surfcoat.2004.09.037
18. Belozerov, V., Sobol, O., Mahatilova, A., Subbotina, V., Tabaza, T. A., Al-Qawabeha, U. F., Al-Qawabah, S. M. (2018). Effect of electrolysis regimes on the structure and properties of coatings on aluminum alloys formed by anodecathode micro arc oxidation. Eastern-European Journal of Enterprise Technologies, 1 (12 (91)), 43–47. doi: https://doi.org/10.15587/1729-4061.2018.121744
19. Subbotina, V. V., Sobol, O. V., Belozerov, V. V., Makhatilova, A. I., Shnayder, V. V. (2019). Use of the Method of Micro-arc Plasma Oxidation to Increase the Antifriction Properties of the Titanium Alloy Surface. Journal of Nano- and Electronic Physics, 11 (3), 03025-1–03025-5. doi: https://doi.org/10.21272/jnep.11(3).03025
20. Belozerov, V., Mahatilova, A., Sobol', O., Subbotina, V., Subbotin, A. (2017). Investigation of the influence of technological conditions of microarc oxidation of magnesium alloys on their structural state and mechanical properties. Eastern-European Journal of Enterprise Technologies, 2 (5 (86)), 39–43. doi: https://doi.org/10.15587/1729-4061.2017.96721
21. Subbotina, V. V., Al-Qawabeha, U. F., Sobol', O. V., Belozerov, V. V., Schneider, V. V., Tabaza, T. A., Al-Qawabah, S. M. (2019). Increase of the α-Al2O3 phase content in MAO-coating by optimizing the composition of oxidated aluminum alloy. Functional Materials, 26 (4), 752–758. doi: https://doi.org/10.15407/fm26.04.752
22. Belozerov, V., Sobol, O., Mahatilova, A., Subbotina, V., Tabaza, T. A., Al-Qawabeha, U. F., Al-Qawabah, S. M. (2017). The influence of the conditions of microplasma processing (microarc oxidation in anodecathode regime) of aluminum alloys on their phase composition. Eastern-European Journal of Enterprise Technologies, 5 (12 (89)), 52–57. doi: https://doi.org/10.15587/1729-4061.2017.112065
23. Clyne, T. W., Troughton, S. C. (2018). A review of recent work on discharge characteristics during plasma electrolytic oxidation of various metals. International Materials Reviews, 64 (3), 127–162. doi: https://doi.org/10.1080/09506608.2018.1466492
24. Xiang, N., Song, R., Zhuang, J., Song, R., Lu, X., Su, X. (2016). Effects of current density on microstructure and properties of plasma electrolytic oxidation ceramic coatings formed on 6063 aluminum alloy. Transactions of Nonferrous Metals Society of China, 26 (3), 806–813. doi: https://doi.org/10.1016/s1003-6326(16)64171-7

25. Lee, J.-H., Kim, S.-J. (2016). Effects of silicate ion concentration on the formation of ceramic oxide layers produced by plasma electrolytic oxidation on Al alloy. Japanese Journal of Applied Physics, 56 (1S), 01AB01. doi: https://doi.org/10.7567/jjap.56.01ab01
26. Javidi, M., Fadaee, H. (2013). Plasma electrolytic oxidation of 2024-T3 aluminum alloy and investigation on microstructure and wear behavior. Applied Surface Science, 286, 212–219. doi: https://doi.org/10.1016/j.apsusc.2013.09.049
27. Liu, C., Liu, P., Huang, Z., Yan, Q., Guo, R., Li, D. et. al. (2016). The correlation between the coating structure and the corrosion behavior of the plasma electrolytic oxidation coating on aluminum. Surface and Coatings Technology, 286, 223–230. doi: https://doi.org/10.1016/j.surfcoat.2015.12.040
28. Borisov, A. M., Krit, B. L., Lyudin, V. B., Morozova, N. V., Suminov, I. V., Apelfeld, A. V. (2016). Microarc oxidation in slurry electrolytes: A review. Surface Engineering and Applied Electrochemistry, 52 (1), 50–78. doi: https://doi.org/10.3103/s106837551601004x
29. Treviño, M., Garza-Montes-de-Oca, N. F., Pérez, A., Hernández-Rodr guez, M. A. L., Juárez, A., Colás, R. (2012). Wear of an aluminium alloy coated by plasma electrolytic oxidation. Surface and Coatings Technology, 206 (8-9), 2213–2219. doi: https://doi.org/10.1016/j.surfcoat.2011.09.068
30. Feng Su, J., Nie, X., Hu, H., Tjong, J. (2012). Friction and counterface wear influenced by surface profiles of plasma electrolytic oxidation coatings on an aluminum A356 alloy. Journal of Vacuum Science & Technology A: Vacuum, Surfaces, and Films, 30 (6), 061402. doi: https://doi.org/10.1116/1.4750474
31. Wan, Y., Wang, H., Zhang, Y., Wang, X., Li, Y. (2018). Study on Anodic Oxidation and Sealing of Aluminum Alloy. International Journal of Electrochemical Science, 13, 2175–2185. doi: https://doi.org/10.20964/2018.02.78
32. Napolskii, K. S., Roslyakov, I. V., Eliseev, A. A., Byelov, D. V., Petukhov, A. V., Grigoryeva, N. A. et. al. (2011). The Kinetics and Mechanism of Long-Range Pore Ordering in Anodic Films on Aluminum. The Journal of Physical Chemistry C, 115 (48), 23726–23731. doi: https://doi.org/10.1021/jp207753v
33. Lee, W. (2010). The anodization of aluminum for nanotechnology applications. JOM, 62 (6), 57–63. doi: https://doi.org/10.1007/s11837-010-0088-5
34. Ardelean, M., Lascău, S., Ardelean, E., Josan, A. (2018). Surface treatments for aluminium alloys. IOP Conference Series: Materials Science and Engineering, 294, 012042. doi: https://doi.org/10.1088/1757-899x/294/1/012042
35. Lu, X., Mohedano, M., Blawert, C., Matykina, E., Arrabal, R., Kainer, K. U., Zheludkevich, M. L. (2016). Plasma electrolytic oxidation coatings with particle additions – A review. Surface and Coatings Technology, 307, 1165–1182. doi: https://doi.org/10.1016/j.surfcoat.2016.08.055
36. Blawert, C., Heitmann, V., Dietzel, W., Nykyforchyn, H. M., Klapkiv, M. D. (2007). Influence of electrolyte on corrosion properties of plasma electrolytic conversion coated magnesium alloys. Surface and Coatings Technology, 201 (21), 8709–8714. doi: https://doi.org/10.1016/j.surfcoat.2006.07.169
37. Shokouhfar, M., Dehghanian, C., Montazeri, M., Baradaran, A. (2012). Preparation of ceramic coating on Ti substrate by plasma electrolytic oxidation in different electrolytes and evaluation of its corrosion resistance: Part II. Applied Surface Science, 258 (7), 2416–2423. doi: https://doi.org/10.1016/j.apsusc.2011.10.064
38. Lv, G., Gu, W., Chen, H., Feng, W., Khosa, M. L., Li, L. et. al. (2006). Characteristic of ceramic coatings on aluminum by plasma electrolytic oxidation in silicate and phosphate electrolyte. Applied Surface Science, 253 (5), 2947–2952. doi: https://doi.org/10.1016/j.apsusc.2006.06.036
39. Ghasemi, A., Raja, V. S., Blawert, C., Dietzel, W., Kainer, K. U. (2010). The role of anions in the formation and corrosion resistance of the plasma electrolytic oxidation coatings. Surface and Coatings Technology, 204 (9-10), 1469–1478. doi: https://doi.org/10.1016/j.surfcoat.2009.09.069
40. Jiang, H., Shao, Z., Jing, B. (2011). Effect of Electrolyte Composition on Photocatalytic Activity and Corrosion Resistance of Micro-Arc Oxidation Coating on Pure Titanium. Procedia Earth and Planetary Science, 2, 156–161. doi: https://doi.org/10.1016/j.proeps.2011.09.026
41. Zong, Y., Cao, G. P., Hua, T. S., Cai, S. W., Song, R. G. (2019). Effects of electrolyte system on the microstructure and properties of MAO ceramics coatings on 7050 high strength aluminum alloy. Anti-Corrosion Methods and Materials, 66 (6), 812–818. doi: https://doi.org/10.1108/acmm-02-2019-2083
42. Borisov, A. M., Krit, B. L., Lyudin, V. B., Peretyagin, P. Y., Suminov, I. V., Apelfeld, A. V. et. al. (2019). Effect of electrolyte composition on electrochemical formation and properties of ceramic-like coatings on aluminum alloys. Journal of Physics: Conference Series, 1281, 012005. doi: https://doi.org/10.1088/1742-6596/1281/1/012005
43. Wu, X., Liu, Q. M., Li, H. X. (2014). Effects of Electrolyte Composition on the Properties of Micro-Arc Oxidation Coatings Formed on 6063 Alloy. Key Engineering Materials, 609-610, 232–237. doi: https://doi.org/10.4028/www.scientific.net/kem.609-610.232
44. Sobol', O. V., Shovkoplyas, O. A. (2013). On advantages of X-ray schemes with orthogonal diffraction vectors for studying the structural state of ion-plasma coatings. Technical Physics Letters, 39 (6), 536–539. doi: https://doi.org/10.1134/s1063785013060126
45. Klopotov, A. A., Abzaev, Yu. A., Potekaev, A. I., Volokitin, O. G. (2012). Osnovy rentgenostrukturnogo analiza v materialovedenii. Tomsk: Izd-vo Tom. gos. arhit.-stroit. un-ta, 276.
46. Besra, L., Liu, M. (2007). A review on fundamentals and applications of electrophoretic deposition (EPD). Progress in Materials Science, 52 (1), 1–61. doi: https://doi.org/10.1016/j.pmatsci.2006.07.001